*Royal Norwegian Council*
*for Scientific and Industrial Research*
*(NTNF)*

NORSAR

NORSAR Scientific Report No. 1-91/92

# Semiannual Technical Summary

## 1 April — 30 September 1991

Kjeller, November 1991

## 7.3 On-line detection using adaptive statistically optimal algorithms

*Background*

In a series of reports (Pisarenko et al, 1987; Kushnir et al, 1989, 1990, 1991), the use of adaptive optimal group filtering (AOGF) for the wideband estimation of seismic signals has been investigated. The method includes autoregressive adaptation to the current noise matrix power spectrum and yields improved noise suppression compared to conventional beamforming, especially at low frequencies where noise power and coherency is highest.

The processes have been implemented in the NORSAR Event Processor (EP) program Package (Fyen, 1989; Kushnir et al, 1991), and comprise adaptive group filtering (AOGF), optimal detection (OD) and optimal onset time estimation (OE).

The main advantage of this signal estimation technique is that it retains an undisturbed signal waveform over a wide frequency band (0.2-5.0 Hz), allowing us to detect and identify signals at frequencies where the noise coherency and power are the greatest. Moreover, when the final decision is to be made on whether the estimated signal is from an earthquake or explosion source, it is important to have a wide-band undisturbed estimate of the signals for discrimination.

The conventional beamforming as an estimator of the signal is together with bandpass filtering a simple and quick process which allows us to detect most interesting signals. However, due to high noise coherence for small arrays, this estimate of the signal will be distorted.

The scope of this report is to analyze the AOGF and OD for the purpose of using the methods in online processing, i.e., continuous processing of all incoming data for a small aperture array like NORESS and ARCESS.

To use AOGF we must do autoregressive adaptation to the noise using a certain time window and a given apparent velocity and azimuth.

We therefore need to investigate how often we need to adapt to the noise and determine how many different aiming points in slowness space we need to be able to detect the signals. Moreover, since the optimal detector (OD) is very sensitive, the threshold to use for acceptable false alarm rates must be carefully considered.

*Automatic Regional Array Processing*

The current on-line detection system uses the STA/LTA detector on conventional bandpass filtered array beams. A large number of different slownesses are used, combined with a number of bandpass filters. The array beams are formed using combinations of sub-geometries of the array.

Considerable gain in noise suppression is obtained by utilizing the negative correlation of the noise wavefield at certain frequencies and inter-sensor distances (Mykkeltveit et al, 1990).

Although the conventional beamforming, filtering and STA/LTA detector scheme work very well, requiring small computer power, there are a few problems that make it reasonable to evaluate the more costly statistical optimal algorithms (SOA) as an alternative online process tool.

1. The STA/LTA detector thresholds and bandpass filters are fixed, so contrary to SOA, it may not take into account the temporary variations in noise coherency and spectrum.
2. As shown by Fyen (1986) and Mykkeltveit et al (1990), the conventional beamforming provides less than $\sqrt{N}$ noise suppression for frequencies below 1 Hz. Therefore the conventional beam detector is used for frequencies only above 1 Hz.
3. The statistical assumptions for the STA/LTA detector to be optimal are not satisfied, which may lead to excessive false alarms and missed detections. The AOGF and OD are based on noise characteristics that better describe the real situation.

We shall here discuss separately the implementation of two algorithms: adaptive statistically optimal group filter (AOGF), here also referred to as adaptive beamformer (AB), and statistically optimal scalar detector (OD), having in mind that the two will be combined as a two-step detector system.

*Time consumption for the detector based on AOGF. Broad band AB deployment.*

The AOGF procedure consists of two steps: adaptation and filtering. Adaptation is the most time consuming and is not realizable in real time (without changing to a recursive adaptive beamformer).

To compute the covariance matrix function and the vector of filter coefficients now takes approximately 5 minutes for 2 minutes of broadband (40 Hz sampling rate) 25-channel data. On the other hand AOGF filtering is rather fast and takes approximately the same time as filtering with Butterworth bandpass filters.

Since the procedure is broken into two individual steps, the adaptation may be performed in parallel to the AOGF, i.e., one process may do noise adaptation (generate the filter) and report this into a data base that may be used by the filter process. So the AOGF processing depends only on how often the parameters of the group filter are to be changed.

In Kushnir et al (1990), it was shown that high noise suppression of AOGF without readaptation remains during at least 40 minutes. On Fig. 7.3.1 the result is shown of AOGF noise suppression without readaptation for 50 hours. Each curve depicted there is the ratio of noise powers P(average channel)/P(AOGF) and P(beam)/P(AOGF). By beam, we mean the conventional array beam - unfiltered.

In this noise study 90 different noise time intervals, each of 2 minute length, were selected by scanning the detection list and requiring that the noise interval started at least 6 minutes after any detection, and at least 6 minutes before any detection.

Adaptation was performed for the 2 minutes in the beginning of this total time interval with the following parameters: frequency band 0.2-1.5 Hz, resampling factor 4, azimuth 334 degrees, velocity 24 km/sec. Subsequently, AOGF filtering was done for these 90 intervals of noise.

Note that the resampling factor 4 means resampling from 40 to 10 Hz, i.e., the adaptation is here done for the frequency range 0.2 - 1.5 Hz, but the output AOGF and conventional beam represent the full frequency range up to the Nyquist frequency (5 Hz).

From Fig. 7.3.1 it is seen that, without readaptation, we get more than 40 times (16 dB) noise suppression compared to an average of single channels.

Some drops in the noise suppression seen on the figure may be related to incoming signals not reported in the detection bulletin, or problems with finding a 'clean' noise interval.

The similar curves were obtained for ARCESS noise with noise adaptation to the frequency bands 0 - 4.5 Hz and 0.2 - 1.5 Hz (Fig. 7.3.2 and 7.3.3).

From the figures it is seen that noise suppression by AOGF is not so stable as for NORESS but nevertheless high noise suppression of more than 16 dB is consistently achieved for more than 6 hours after adaptation.

The stability of AOGF noise suppression in time may be explained by the fact that the adaptation is done in the lower frequency bands where noise power fluctuations are smallest (Fyen, 1990).

Let us consider now the possibilities of constructing a small array detector system consisting of several adaptive beams steered at certain azimuths and velocities. Such a system will be analogous to the on-line NORESS detector system.

The main question here is: what is the minimum number of AB providing adequate detectability while still allowing real-time or routine processing.

To try to answer this question, an experiment was performed with simulating events of different SNR - signal to noise ratio. A strong regional event with Pn parameters: azimuth 193, velocity 8.2, frequency band 2.5-4.5 Hz, SNR 148, was selected. This event was treated as a signal without noise, and then scaled down and added to arbitrary NORESS noise. Figures 7.3.4 and 7.3.5 show the results. The 5 curves in each figure correspond 'events' of 5 different SNR as function of slowness of the AOGF beam. For each chosen azimuth and velocity, adaptation was done for 120 seconds of preceding pure noise, followed by filtering of the signal segment by AOGF (i.e., forming an AOGF beam). The curves show SNR for the AOGF beam (SNROGF) and the corresponding single channel A0 maximum SNR for each different scale of the signal. SNR was estimated by the ratio of STA of the 2 first seconds of the signal and average STA of 40 sec of pure noise.

From the figures we see that we get highest SNR of the AOGF at the correct azimuth, whereas SNR is nearly constant for velocities above 6 km/sec. Looking at the shape of the SNR curve for azimuth, we see for azimuth range 150 - 225 degrees, the SNR varies by a factor of two.

Allowing a predefined beam set to have a worst case missteering loss of 3 dB, we may infer that 8 different azimuths and two velocities may be enough to produce high detectability for all azimuths and velocities. That is, 16 noise adaptations has to be performed at regular intervals separated up to 6 hours. This will be an acceptable load for most systems.

*Frequency dependence of noise suppression for AOGF and standard beams. Low frequency AOGF deployment.*

The current NORESS detector system was designed mainly for the detection of local and regional events, having its best performance in the high frequency band (>2 Hz). But as it was shown by Ringdal (1990), it is very effective also for the detection and reporting of teleseismic signals.

Most of the teleseismic events detected at NORESS are from the Eurasian continent having the best properties of propagation at high frequencies (1.5 - 4 Hz). But for teleseismic signals coming from other directions, energy at these frequencies attenuate much more strongly. As a result, much of the teleseismic information is masked by low frequency noise and this reduces the detectability of the current operational system.

We shall try to show that complementing the current detector system with SOA may improve the detectability also for teleseismic distances. Let us compare noise suppression by AOGF and standard beams in different frequency bands reflected in Table 7.3.1. By a standard beam we mean one of the conventional beams used in NORESS/ARCESS online system. Such a standard beam is defined by array sub-configuration, velocity and azimuth. Sub-configurations are denoted in such a way that, e.g., A0AC, means the center instrument A0, plus the A-ring and C-ring.

The table comprises STA values evaluated on pure NORESS noise using AOGF and standard beam traces filtered in the most important frequency bands, that is, the AOGF as the result of the group filtering is additionally filtered with the same bandpass filters as the standard beams. The AOGF was based on noise adaptation in the frequency band 0-16 Hz. As STA is an estimate of the power, the table is also indicative of the absolute level of noise suppression.

For AOGF, the 25 vertical NORESS channels (A0ABCD configuration) were used. Noise adaptation was performed using a 100-second noise segment preceding the 40 seconds of data used for beams and AOGF filtering. For these teleseismic AOGF and standard beams, infinite velocity and zero azimuth was used.

From the table it is seen that:

1. In all of the listed frequency bands, the resulting noise power of AOGF is lower than the standard beams, i.e., better noise suppression is obtained.

2. The best standard beam configurations were A0D for 0.3-1.0 Hz and 0.5-1.5 Hz, and A0CD for 1.5-5.0 Hz and 5-16 Hz.
3. Compared to the A0D beam, broadband AOGF has 10 dB better suppression in the 0.3-1.0 Hz and 6 dB improvement in the 0.5-1.5 Hz frequency bands.
4. In the highest frequency band the AOGF and A0CD have comparable noise suppression results.
5. As the highcut frequency of the lowpass prefiltering in the noise adaptation (lowpass 16 Hz in the first part of the table) decreases, the STA power of AOGF also decreases, that is, noise suppression improves.

For a lowpass (lp) 1.5 Hz filter, the AOGF shows approximately 6 dB smaller STA value for the 0.3-1.0 Hz and 0.5-1.5 Hz bands, as opposed to adaptation with lp 16 Hz. In the band 0.2-0.6 Hz, comprising a considerable part of the noise power, the AOGF is suppressed 19 dB compared to A0D.

Hence, the best teleseismic performance of AOGF is achieved by prefiltering the data with a low pass filter 1.5 Hz

*Comparison of optimal detector and STA/LTA detectability*

We will here present some preliminary results concerning application of the one-dimensional statistically optimal detector, i.e., the so-called ESTDET algorithm (Kushnir et al, 1991). This algorithm is based on optimal accounting of noise features. Compared to the ordinary STA/LTA algorithm, this algorithm not only takes into account amplitude level, but also variations of the spectrum content.

The procedure has two steps: The first is adaptation on a time segment of pure noise. As a result we get an estimate of whitening filter coefficients. The second step is filtering using the coefficients computed at the previous step and computation of Chi-square statistic in a moving window.

To examine the performance of ESTDET as a function of SNR, we have chosen a NORESS recording of a regional event in Sweden, i.e., the same event used for Fig. 7.3.4.

The event was detected with relatively high SNR by standard beam N055 (configuration A0BCD, frequency band 2.5-4.5 Hz). Again we used the procedure of superposing this signal onto pure NORESS noise with different scaling.

Fig. 7.3.6 shows the display of the bandpass filtered beam N055, the STA for this beam, and ESTDET (XISQT1 Chi-square statistics from ESTDET process) for this original signal. The lower part of the figure shows the same three processes when the signal is scaled down by a factor 80 in amplitude and added to a noise trace.

The advantage of ESTDET over STA for the latter case is obvious.

The next experiment was to obtain ESTDET statistics with varying noise scale factors for the simulated data.

The ESTDET statistic was computed for the AOGF beam and for the standard beam. Signal-to-noise ratio was estimated by the ratio of ESTDET for the 3 first seconds of P-wave and 40 seconds of preceding pure noise, i.e. Xi-square values are averaged for the noise segment to get a signal-to-noise ratio comparable to STA/LTA. For the standard beam, the STA was used.

Fig. 7.3.7 shows the results. The upper curve is the ratio of ESTDET statistic maxima on signal and noise. The curve is computed for unfiltered AOGF data. The bottom curve is the corresponding ratio for the STA algorithm (SNR) on standard beam N055. This ratio estimates STA/LTA. The middle curve is similar to the upper one, but additionally band-pass filtered in the frequency band 2.5-4.5 Hz.

Comparing upper and bottom curves, it is seen that the ESTDET SNR is better than that of the STA/LTA algorithm, especially for the unfiltered AOGF beam. For example, for noise scale equal to 100, SNR for STA is 2 and for ESTDET is 50-60.

To examine ESTDET false alarms we have chosen from two days bulletin all noise intervals of at least 2 minutes length and selected 2 minutes segments from each. The total amount of noise is about 3 hours.

Fig. 7.3.8 shows the number of ESTDET values exceeding a given threshold, as a function of threshold. For low thresholds it is very large, but it decreases with increasing of the threshold value. Only one exceedance is detected for a threshold larger than 500. Let us compare it with the maximum values of ESTDET on the signal+noise (Fig. 7.3.9) computed for different noise scales. It is seen that value 500 corresponds to a noise scale of 85 or STA/LTA value around 2 which is lower than the conventionally used threshold.

So, we may suppose that if the threshold for ESTDET is equal to, say, 550, it is possible to detect a weak regional P-wave, STA/LTA=2, with a low probability of false alarms during several hours of processing.

From these preliminary results we may draw the following conclusions:

1. AOGF is computed after adaptation to the noise. This process is time consuming, but it is shown that high noise suppression may be obtained using only one noise adaptation for several hours of data processing.
2. It has been shown that for a NORESS-type array adaptation to the noise for about 8 different azimuths and two velocities, is sufficient to obtain adequate beam coverage for regional P phases.
3. The main advantage of AOGF is to be expected for low frequency teleseismic signals, where we have both good detectability and a broadband undisturbed estimate of the signal.

4. The ESTDET detector is much more sensitive to the detection of seismic phases compared to conventional STA/LTA due to optimal accounting to noise spectrum variations.
5. Due to higher sensitivity the ESTDET process may be used for the detection and timing of much weaker seismic phases than detected now.

**V. Pinsky, MITPAN Institute, Moscow**
**S. Tsvang, MITPAN Institute, Moscow**
**J. Fyen**

## References

Fyen, J., (1989): Event processor program package. *Semiannual Technical Summary*, NORSAR Sci. Rep. 2-88/89, Kjeller, July 1989.

Fyen, J., (1986): NORESS noise spectral studies - beam suppression. *Semiannual Technical* Summary, NORSAR Sci. Rep. 1-86/87, Kjeller, November 1986.

Fyen, J., (1990): Diurnal and seasonal variations in the microseismic noise level observed at the NORESS array. *Physics of the Earth and Planetary Interiors*, 63: 252-268.

Kushnir, A.F., V.I. Pinsky and J. Fyen (1989): Statistically optimal event detection using small array data. *Semiannual Technical Summary*, NORSAR Sci. Rep. 1-89/90, Kjeller, December 1989.

Kushnir, A.F., V.I. Pinsky, S. Tsvang, J. Fyen, S. Mykkeltveit and F. Ringdal (1990): Optimal group filtering and noise attenuation for the NORESS and ARCESS array. *Semiannual Technical Summary*, NORSAR Sci. Rep. 1-90/91, Kjeller, November 1990.

Kushnir, A.F., J. Fyen and T. Kværna (1991): Multichannel statistical data processing algorithms in the framework of the NORSAR event processing program package. *Semiannual Technical Summary*, NORSAR Sci. Rep. 2-90/91, Kjeller, May 1991.

Kushnir, A.F., V.M. Lapshin, V.I. Pinsky and J. Fyen (1990): Statistical optimal event detection using small array data. *Bull. Seism. Soc. A*m., Vol. 80, No. 6, pp. 1934-1950, December 1990.

Mykkeltveit, S., J. Fyen, F. Ringdal and T. Kværna (1990): Spatial characteristics of the NORESS noise field and implications for array detection processing. *Physics of the Earth and Planetary Interiors*, 63: 277-283.

Pisarenko, V.F, A.F. Kushnir and I.V. Savin (1987): Statistical adaptive algorithms for estimations of onset moments of seismic phases. *Phys. Earth Planet. Inter.*, 47, 4-10.

Ringdal, F. (1990): Teleseismic event detection using the NORESS array, with special reference to low-yield Semipalatinsk explosions. *Bull. Seism. Soc. Am.*, Vol. 80, No. 6, pp. 2127-2142, December 1990.

Adaptation lp 16 Hz

| Filter band | AOGF | A0ABCD | A0BC | A0D | A0CD | A0AB | A0 |
|---|---|---|---|---|---|---|---|
| 0.3 - 1.0 Hz | 0.035 | 0.150 | 0.188 | 0.105 | 0.131 | 0.206 | 0.207 |
| 0.5 - 1.5 Hz | 0.044 | 0.142 | 0.192 | 0.085 | 0.114 | 0.219 | 0.226 |
| 1.5 - 5.0 Hz | 0.018 | 0.038 | 0.062 | 0.032 | 0.022 | 0.093 | 0.113 |
| 5.0 - 16.0 Hz | 0.005 | 0.0056 | 0.0076 | 0.065 | 0.0071 | 0.0094 | 0.027 |
| Unfiltered | 0.05 | 0.174 | 0.225 | 0.157 | 0.145 | 0.256 | 0.271 |

**Adaptation lp 4.5 factor 4**

| | |
|---|---|
| 0.3 - 1.0 Hz | 0.023 |
| 0.5 - 1.5 Hz | 0.029 |
| 1.5 - 5.0 Hz | 0.016 |
| Unfiltered | 0.034 |

**Adaptation lp 1.5 factor 4**

| | | | |
|---|---|---|---|
| 0.2 - 0.6 Hz | 0.011 | 0.090 | 0.139 |
| 0.3 - 1. Hz | 0.019 | | |
| 0.5 - 1.5 Hz | 0.023 | | |
| Unfiltered | 0.025 | | |

**Table 7.3.1.** Comparison of AOGF noise suppression in different frequency bands.Case study of NORESS noise segment start 1991-140:00.05.00.004. The table shows STA power values (normalized with factor 1000) for AOGF and different standard beams. AOGF adaptation using velocity 99999, azimuth 0.0, lowpass 16 Hz prefilter and 100 seconds noise. Data are not resampled (resample factor 1). STA power values on the following 40 seconds. Before STA, traces are butterworth bandpass filtered in the given filter bands. A0BC, etc., show which sub-configuration that is used. Additional values are computed for AOGF using lowpass 4.5 and 1.5 Hz and resampling factor 4. (Resample from 40 to 10 Hz).

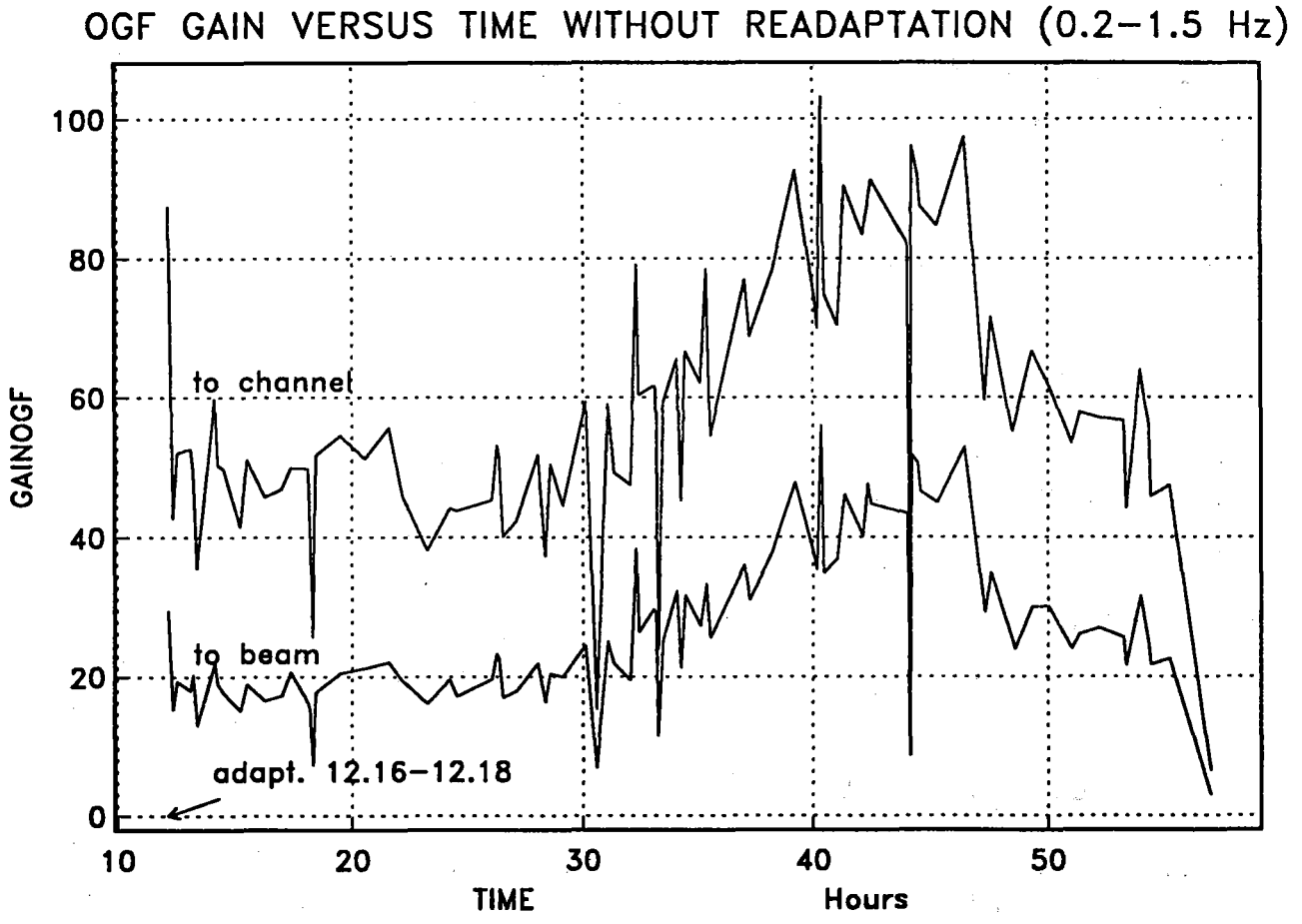


**Fig. 7.3.1.** AOGF gain versus time without readaptation on pure NORESS noise selected from bulletin. OGFGAIN is the ratio of noise powers on 2-minute noise intervals. Start time 1991-176:12. Adaptation interval 1991-176:12.16 - 12.18. Data frequency band 0.2-1.5 Hz. Adaptation velocity 24 km/sec, azimuth 334 degrees.

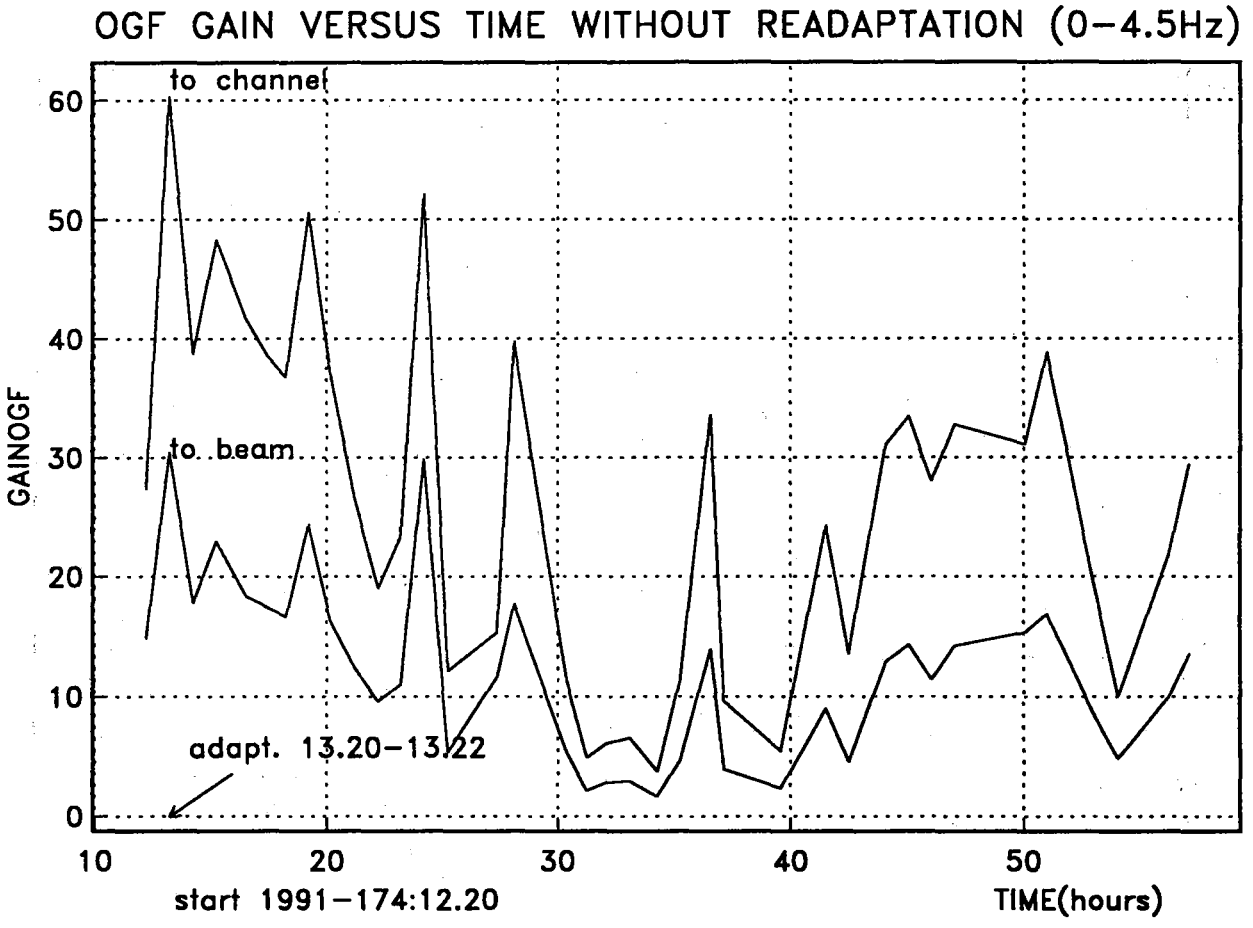


**Fig. 7.3.2.** AOGF gain versus time without readaptation on pure ARCESS noise selected from bulletin. OGFGAIN is the ratio of noise powers on 2-minute noise intervals. Start time 1991-174:12.20 Adaptation interval 1991-176:13.20 - 13.22. Data frequency band 0-4.5 Hz. Adaptation velocity 10 km/sec, azimuth 193 degrees.

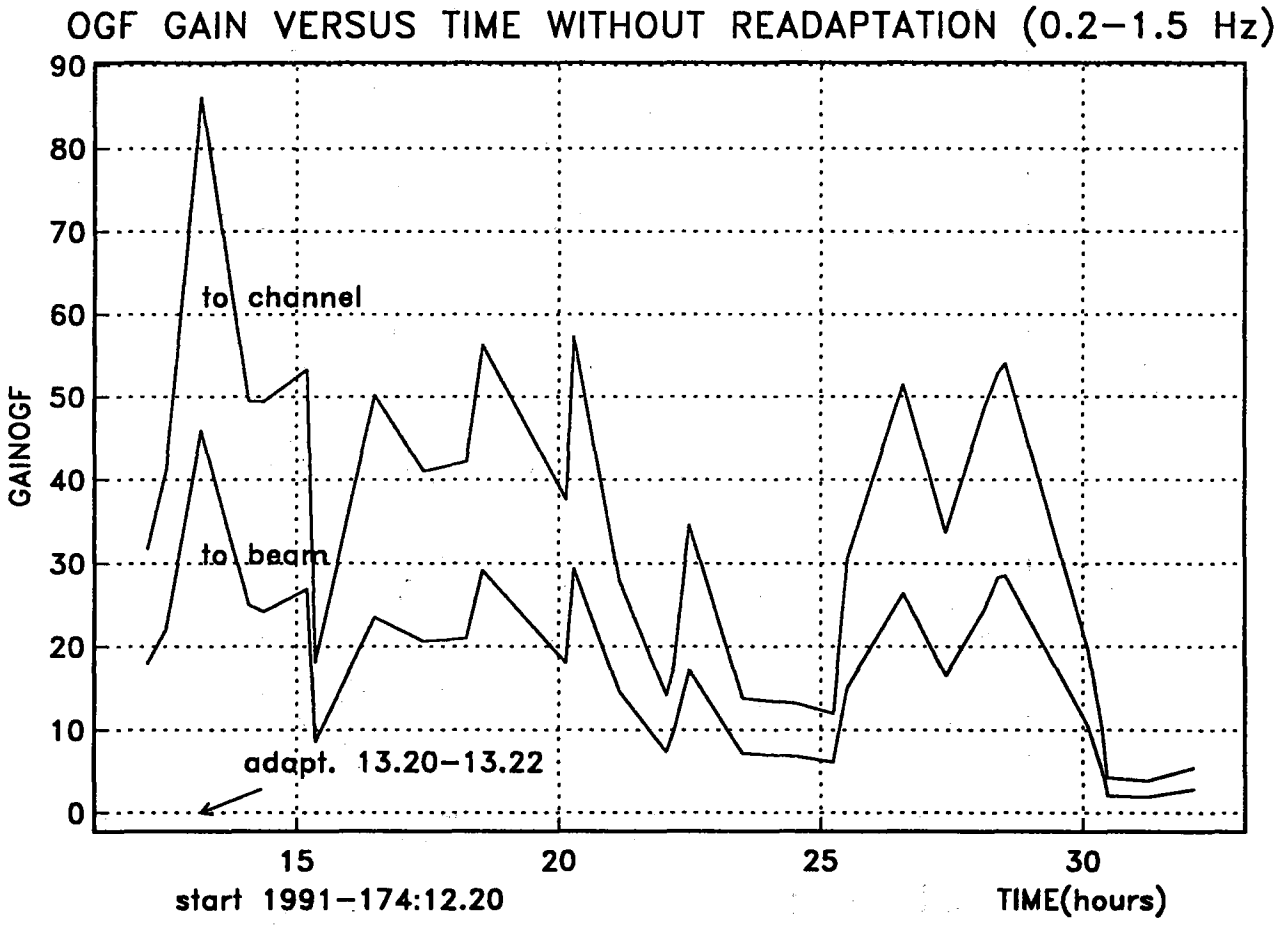


**Fig. 7.3.3.** AOGF gain versus time without readaptation on pure ARCESS noise selected from bulletin. OGFGAIN is the ratio of noise powers on 2-minute noise intervals. Start time 1991-174:12.20 Adaptation interval 1991-176:13.20 - 13.22. Data frequency band 0.2-1.5 Hz. Adaptation velocity 10 km/sec, azimuth 193 degrees.

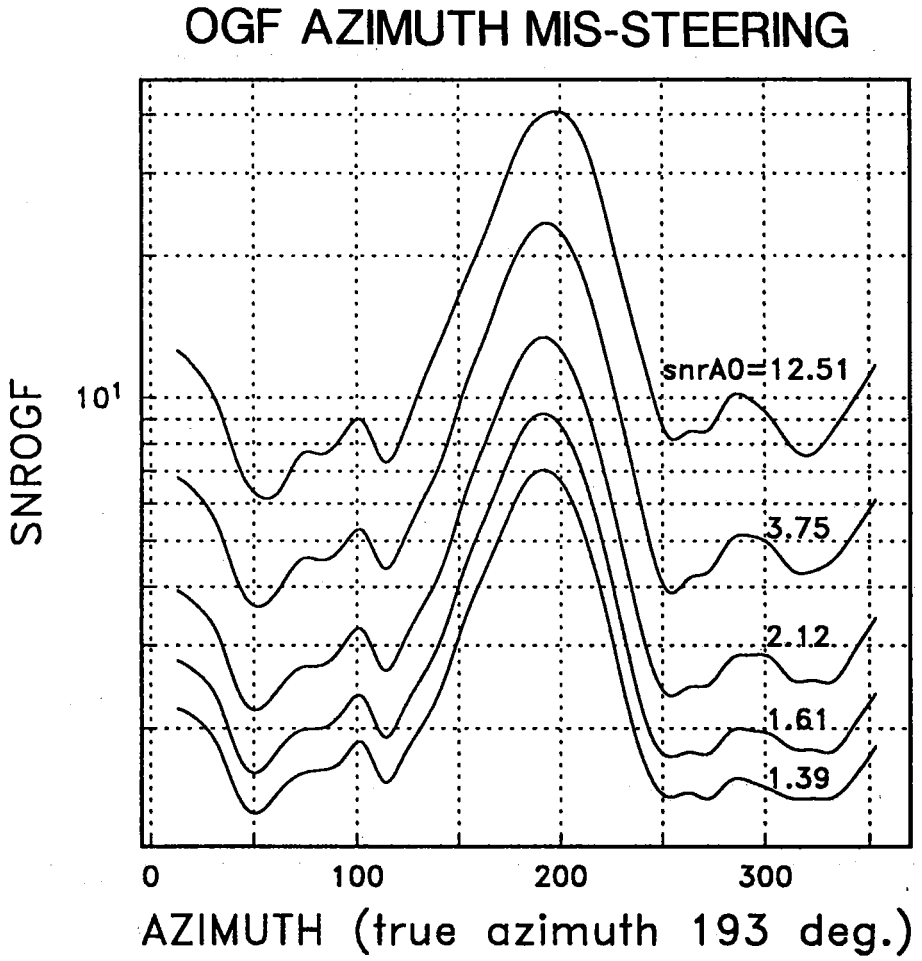


**Fig. 7.3.4.** AOGF azimuth missteering on regional event NORESS P-wave with different scaling of added noise. Signal parameters: start 1991-086:05.18.46, velocity 8.2 km/sec azimuth 193 degrees, freq. 3.35 Hz. Noise start 1991-140:00.05. OAGF adaptation on 100 seconds of pure noise with velocity 8.2 km/sec, frequency band: 0-4.5 Hz, and different azimuths. Filtering on 50 seconds of signal + noise. SNROGF= (average STA on 2 sec. of P-wave)/(average STA on 40 sec. of noise)

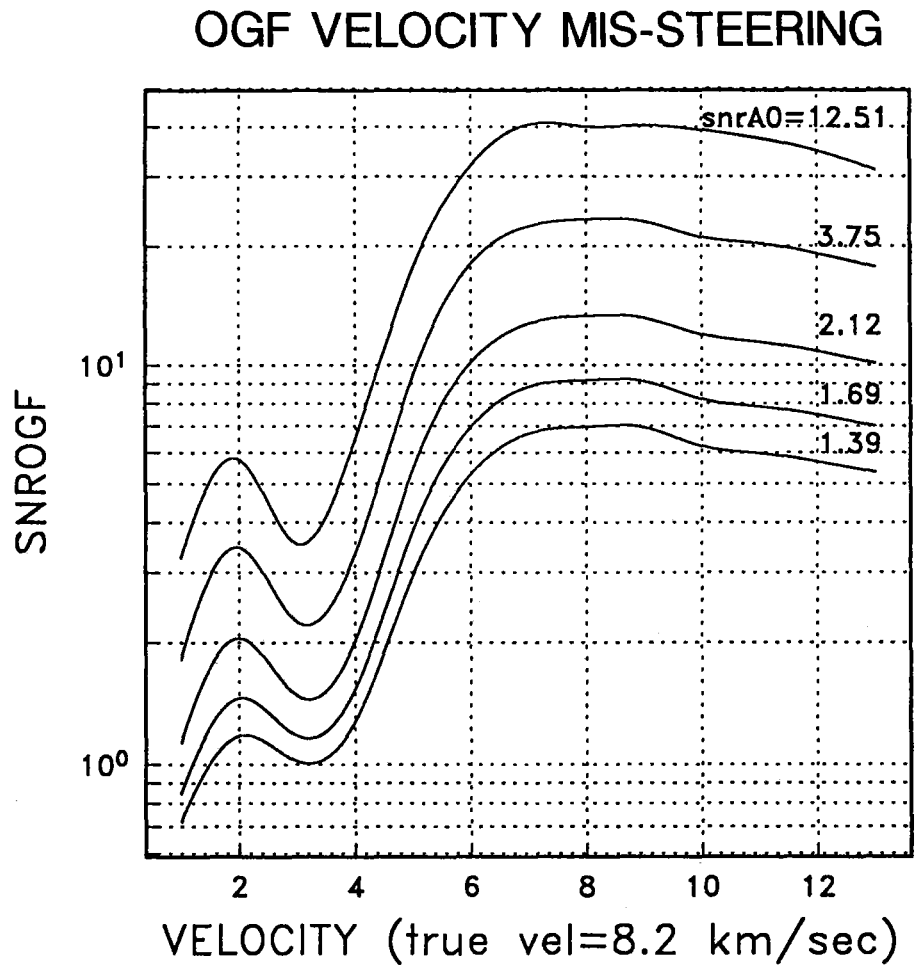


**Fig. 7.3.5.** AOGF velocity missteering on regional event NORESS P-wave with different scaling of added noise. Signal parameters: start 1991-086:05.18.46, velocity 8.2 km/sec azimuth 193 degrees, freq. 3.35 Hz. Noise start 1991-140:00.05. OAGF adaptation on 100 seconds of pure noise with azimuth 193 degrees, frequency band: 0-4.5 Hz and different velocities. Filtering on 50 seconds of signal + noise. SNROGF= (average STA on 2 sec. of P-wave)/(average STA on 40 sec. of noise)

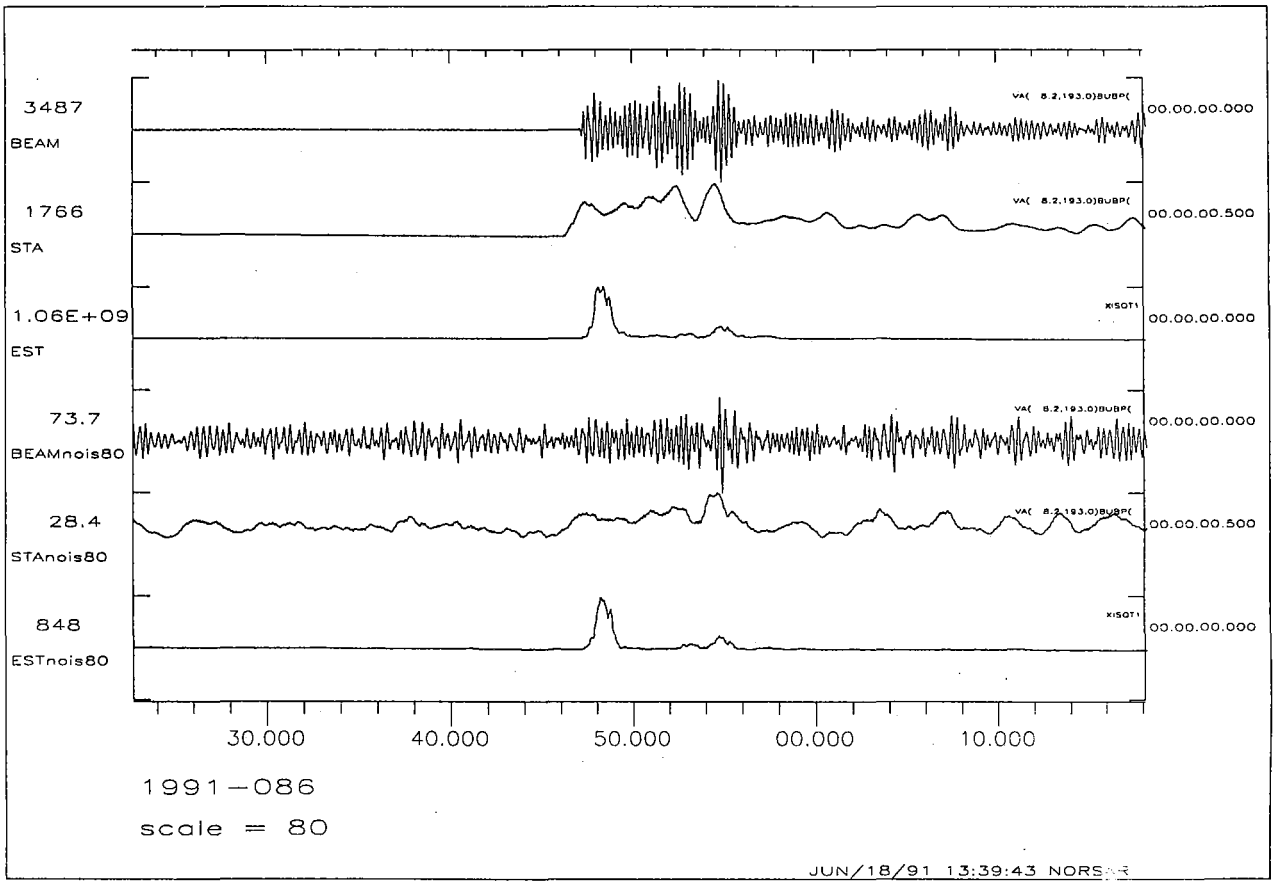


**Fig. 7.3.6.** STA for ESTDET and standard beam n055 for regional event. Signal parameters: start 1991-086:05.18.46, velocity 8.2 km/sec azimuth 193 degrees, freq. 3.35 Hz. Noise start 1991-140:00.05. Traces: 1. standard bean (SB), fr.band 2.5-4.5 Hz; 2. STA on SB; 3. ESTDET on SB; 4. SB + noise,scale=80; 5.,6. STA and ESTDET on SB + noise.

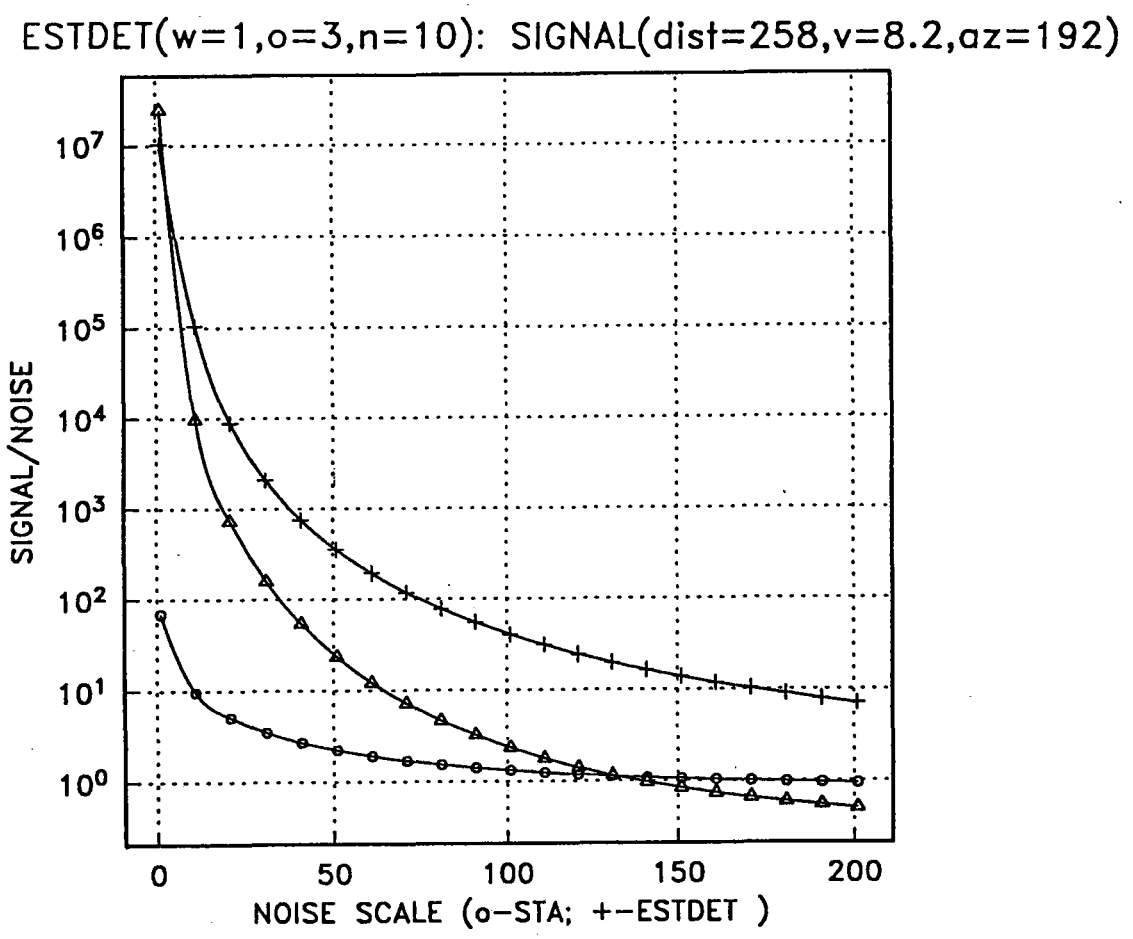


**Fig. 7.3.7.** Comparison of ESTDET and STA/LTA on the regional P-phase + noise for the different noise scales. ESTDET parameters: (w=1,o=3,n=10).

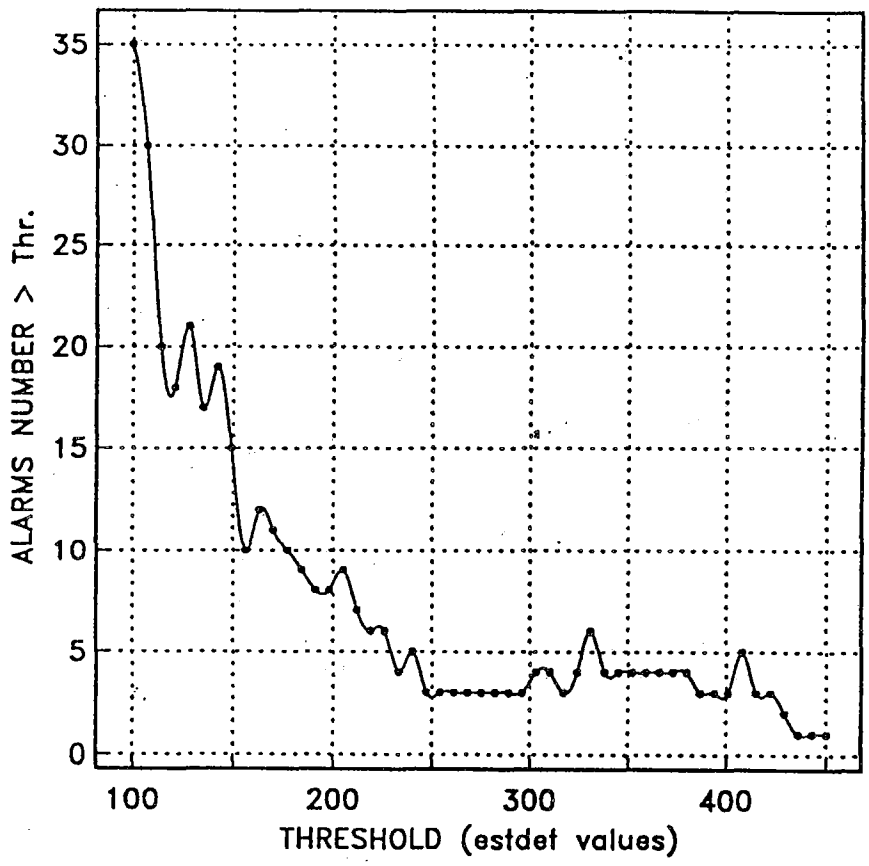


**Fig. 7.3.8.** Number of ESTDET false alarms versus threshold for 3 hours of NORESS noise taken from 48 operational hours.

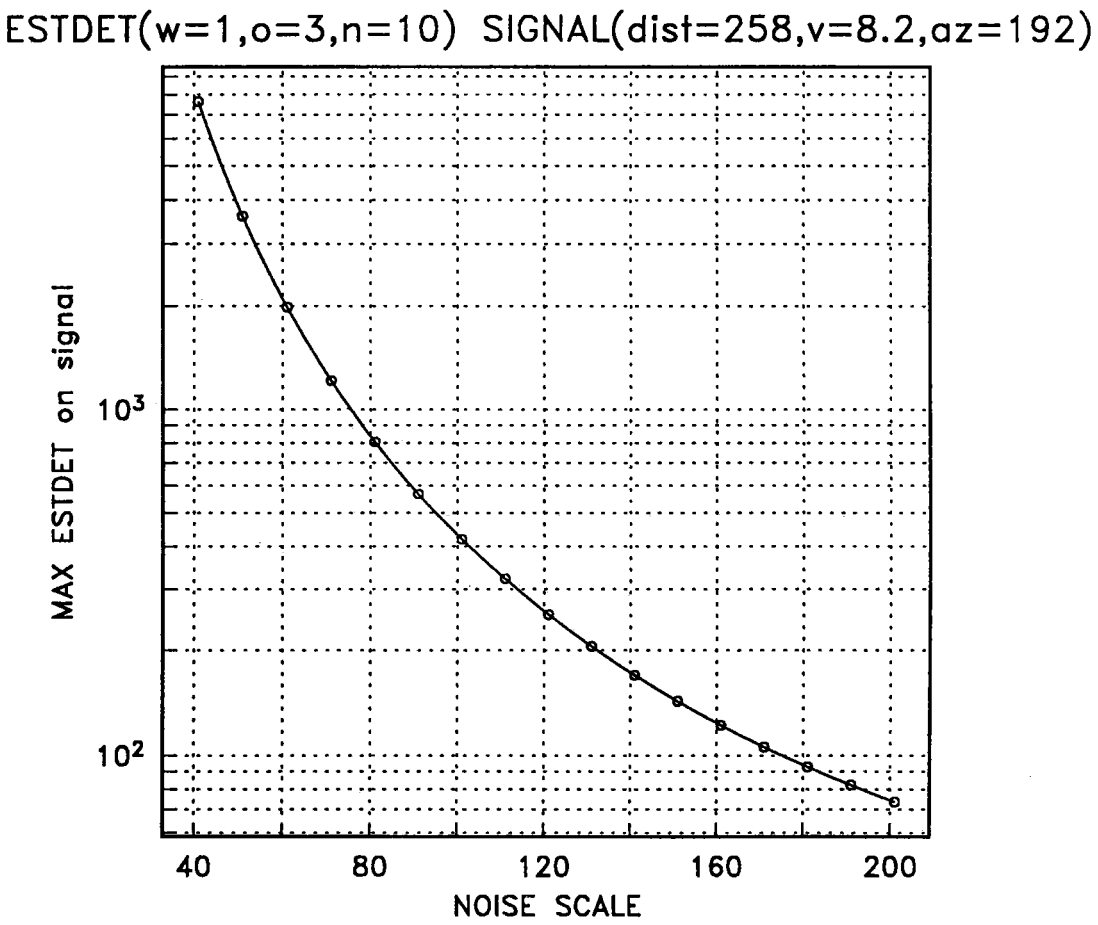


**Fig. 7.3.9.** Maximum values of estdet on regional P-phase + noise versus noise scale.